The EOS of dense matter from effective field theory interactions

Kai Hebeler

Darmstadt, February 25, 2021

with Jonas Keller, Christian Drischler, Corbinian Wellenhofer and Achim Schwenk

PHAROS WOrkshop:
Neutron star equation of state and transport properties

SFB 1245

TECHNISCHE UNIVERSITÄT DARMSTADT

Chiral effective field theory for nuclear forces

power-counting:
expand in Q/Λ, error estimates!

degrees of freedom:
nucleons and pions

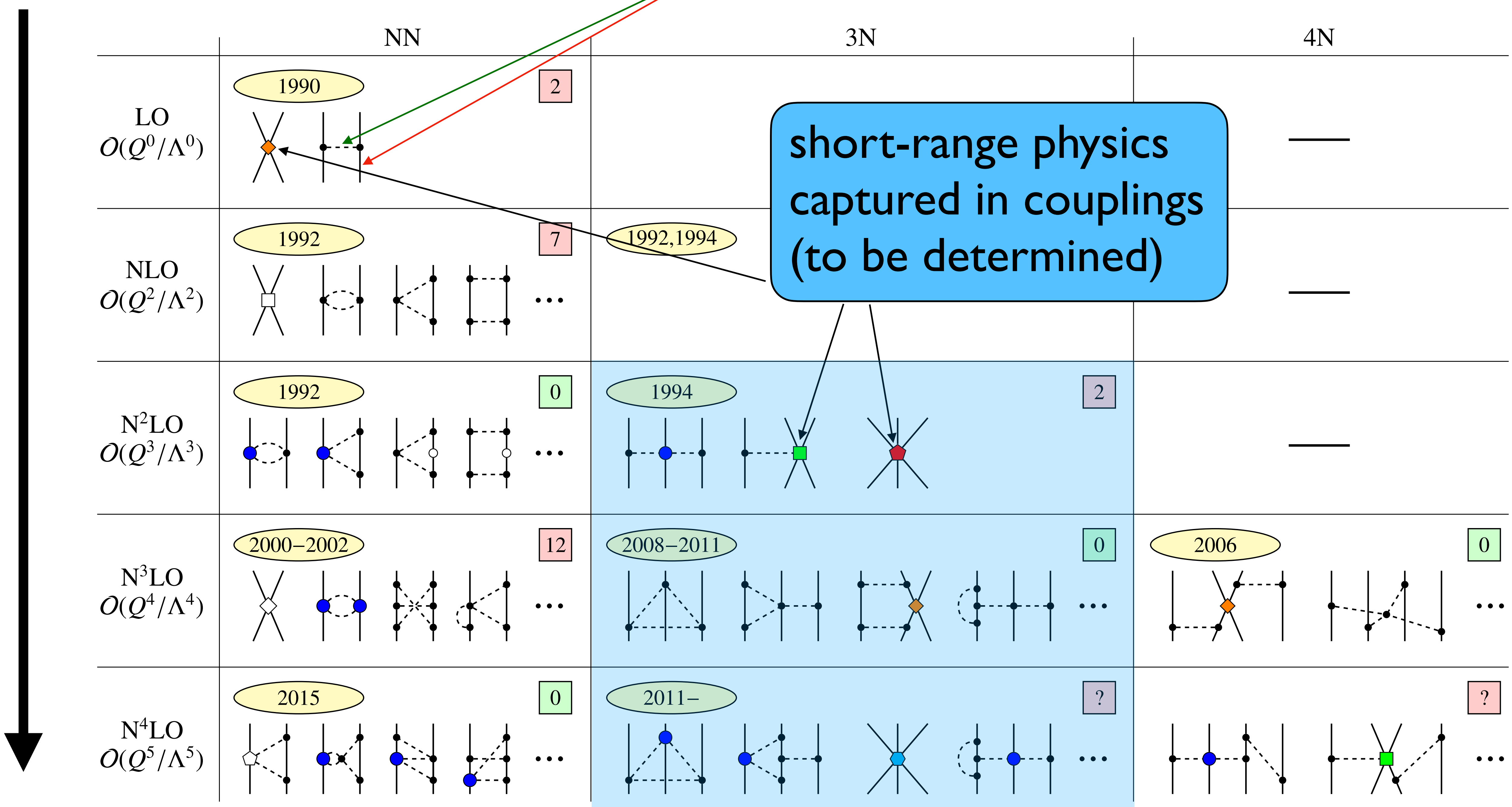

short-range physics
captured in couplings
(to be determined)

3N forces appear naturally

KH, Phys. Rept. 890, 1 (2021)
KH, Krebs, Epelbaum, Golak, Skibinski,
PRC 91, 025805 (2015)

Development of nuclear interactions

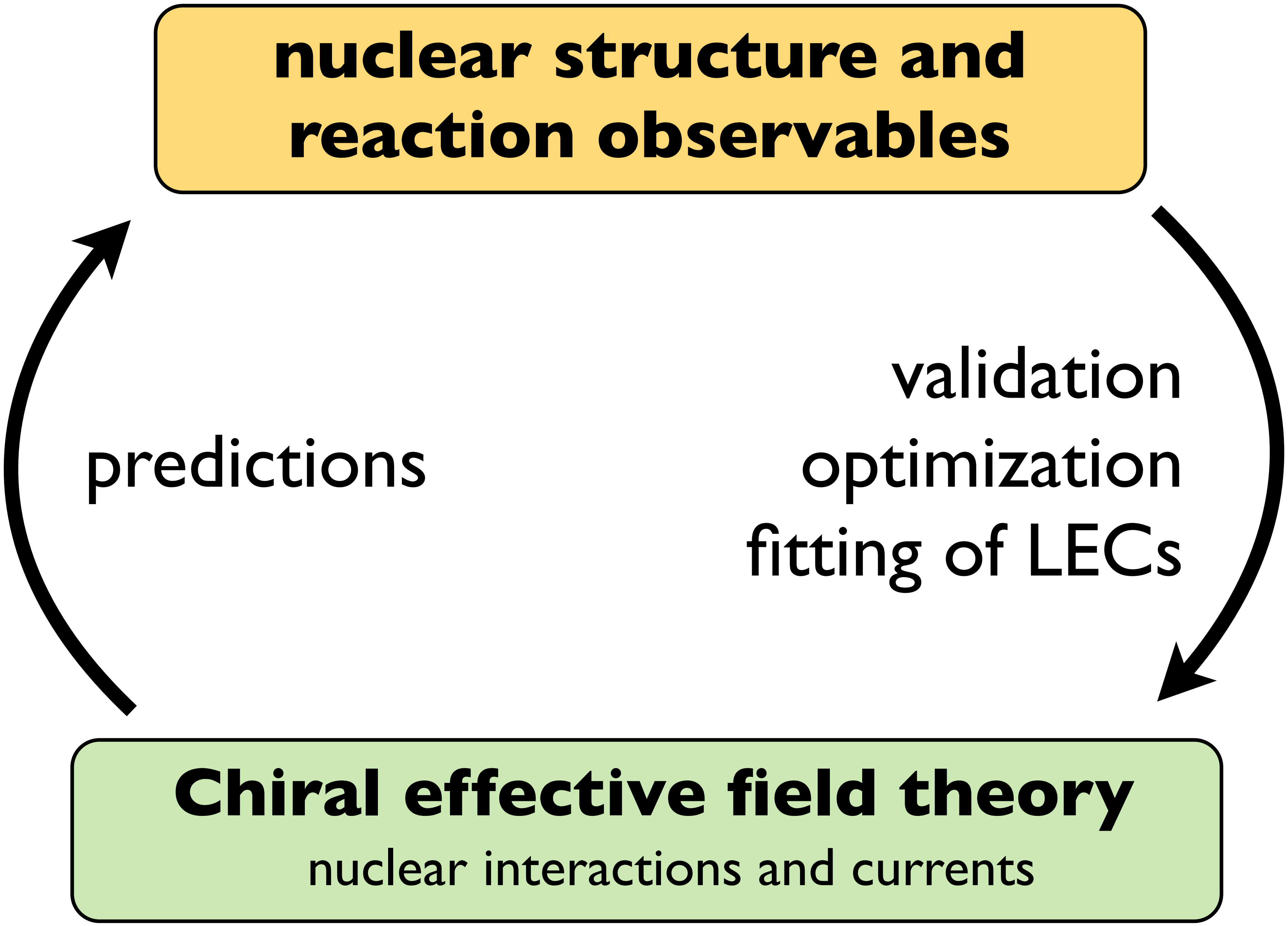

Systematically changing the resolution: the Similarity Renormalization Group

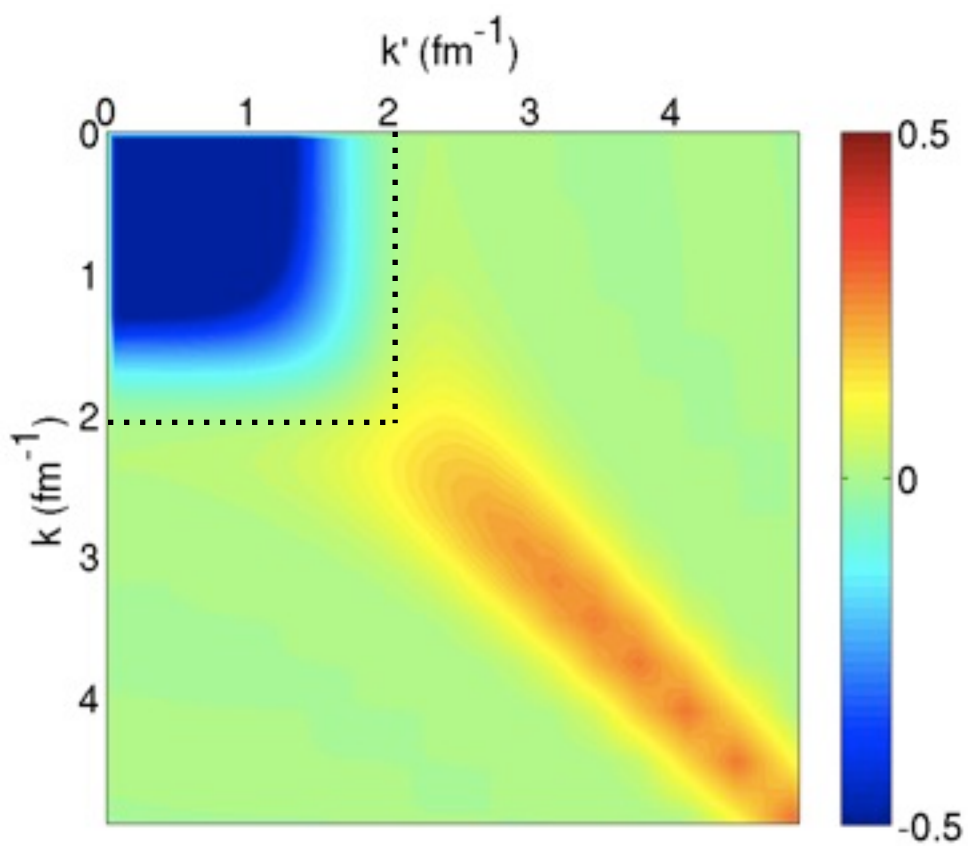

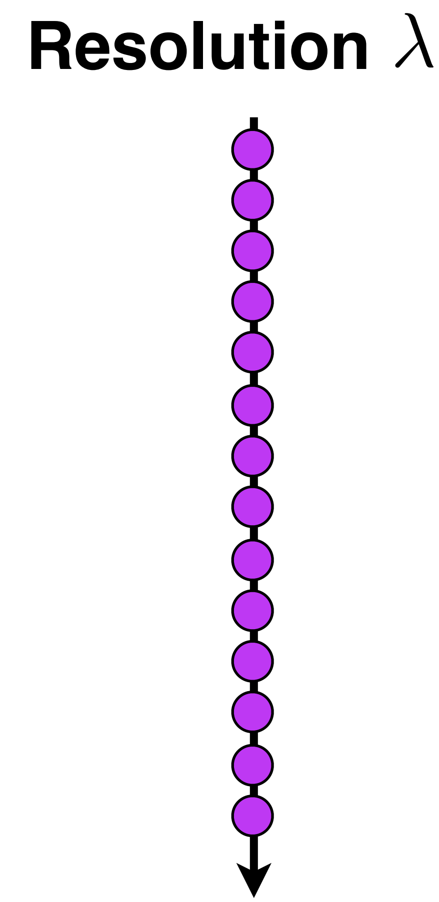

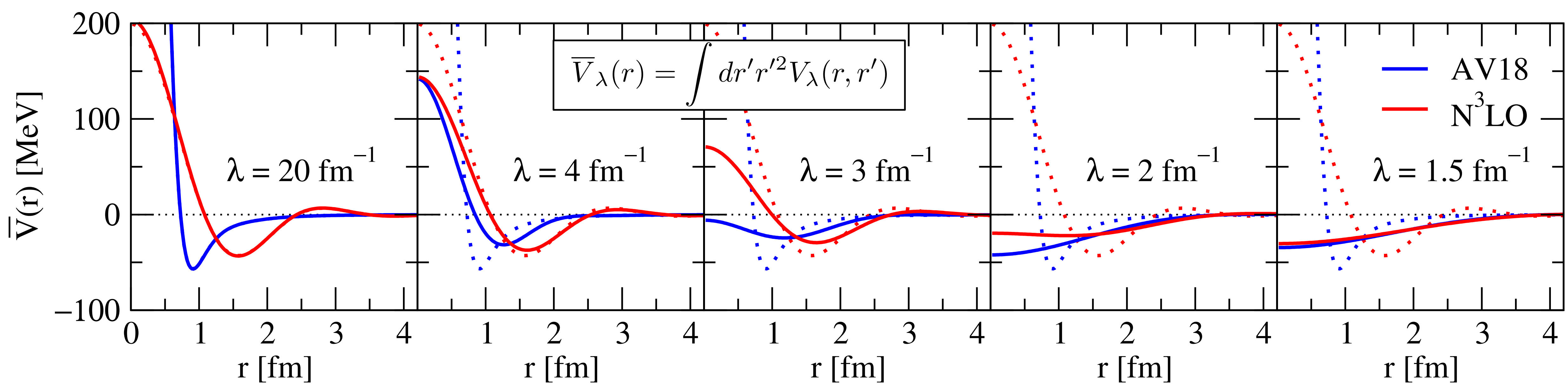

Wendt et al., PRC 86, 014003 (2012)

Equation of state of symmetric nuclear matter: nuclear saturation

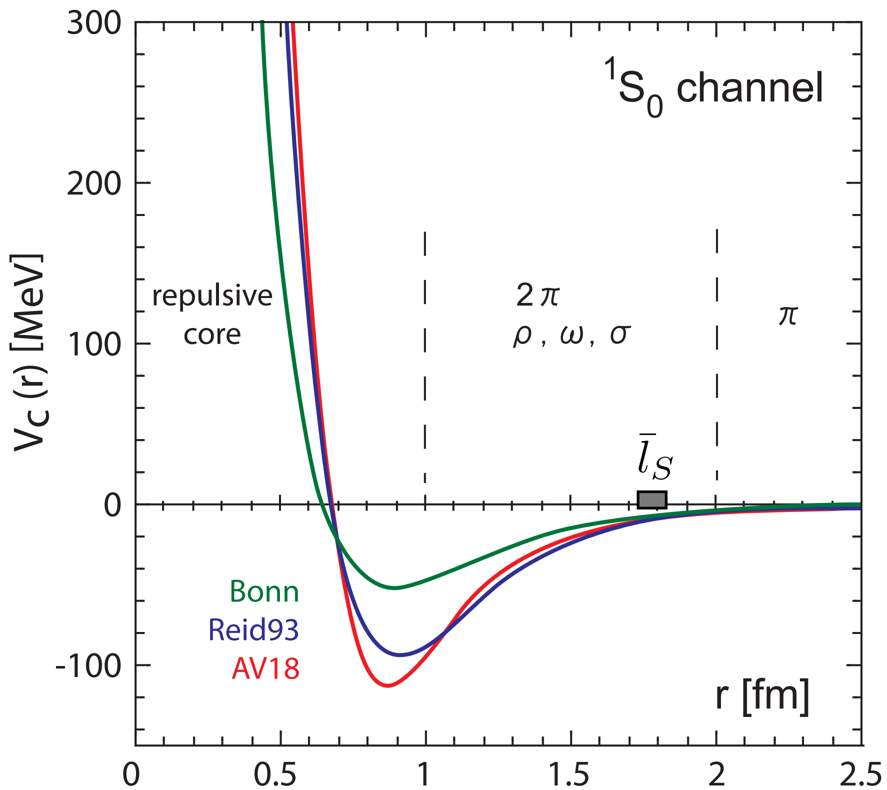

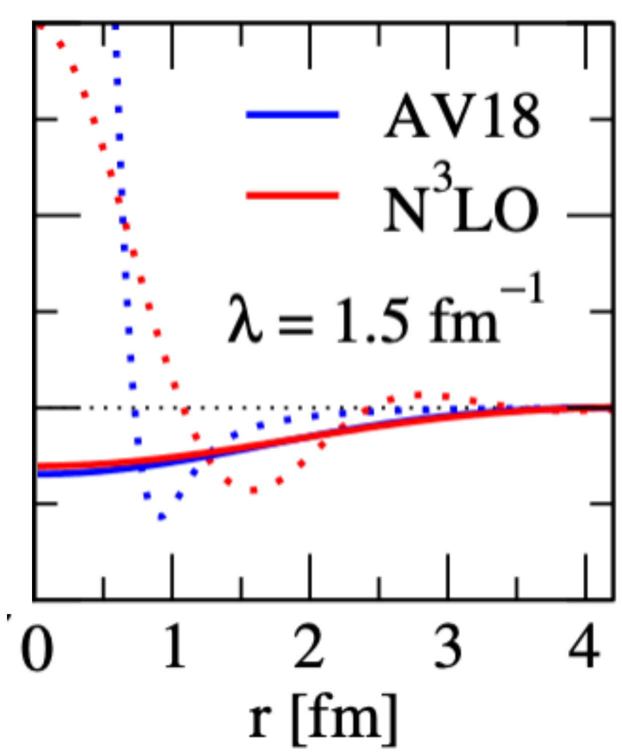

Batty et. al,
Karlsruhe (1987)

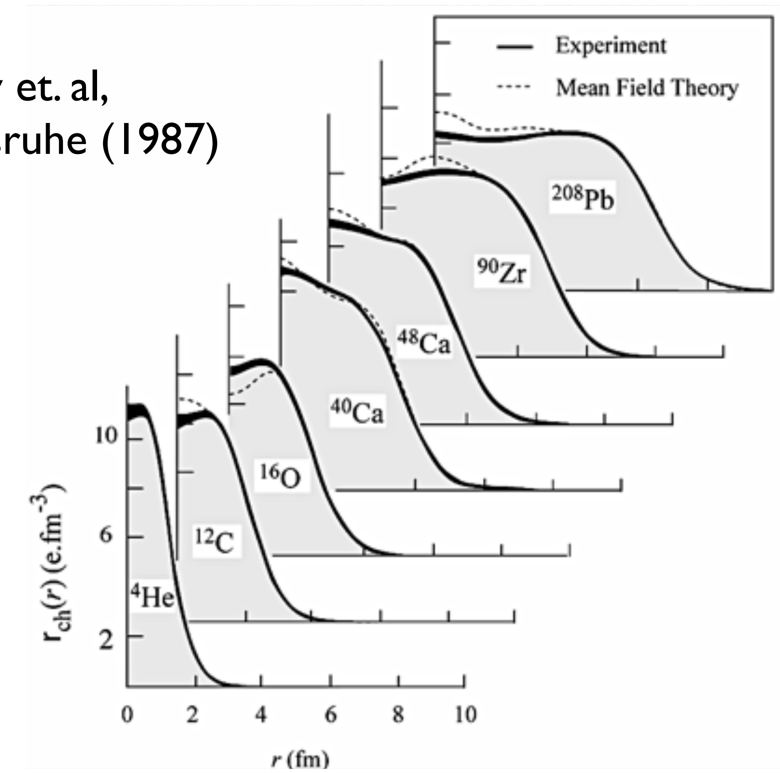

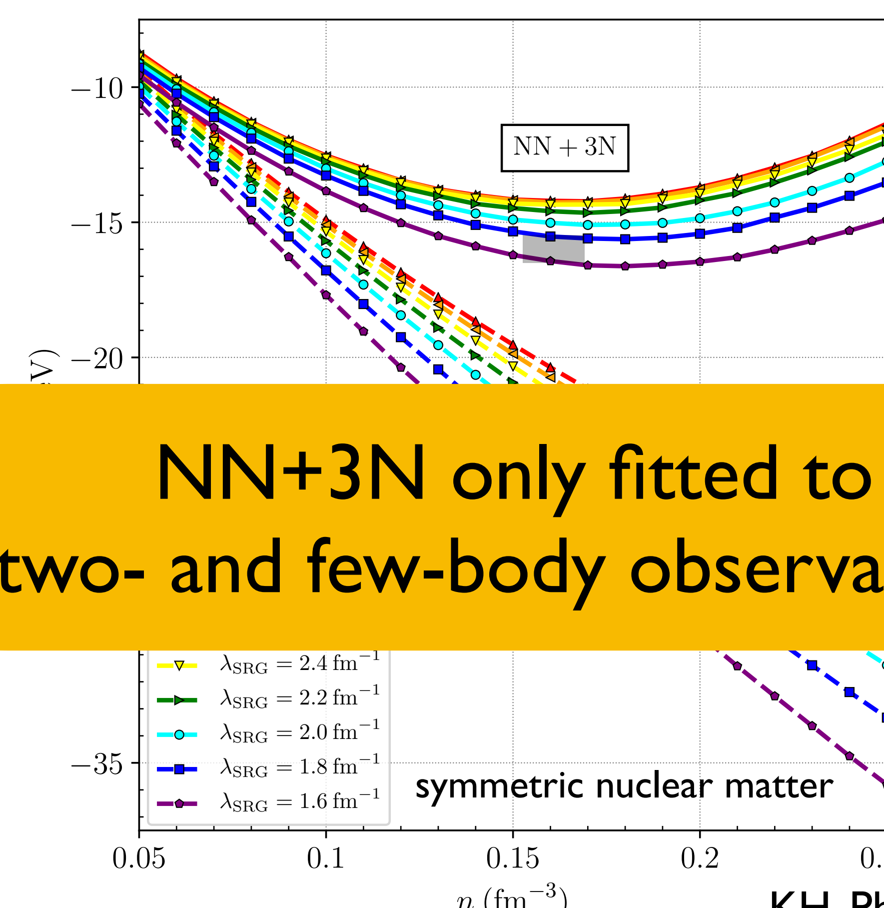

NN+3N only fitted to
two- and few-body observables!

KH, Phys. Rept. 890, 1 (2021)

Novel efficient many-body perturbation theory framework for nuclear matter

Problem:

Evaluation of MBPT diagrams beyond second order in perturbation theory becomes complicated and tedious in partial wave representation.

Strategy:

Implementation of NN and 3N forces without partial wave decomposition.

Calculate MBPT diagrams in vector basis

$$|12...n\rangle = |\mathbf{k}_1 m_{s_1} m_{t_1}\rangle \otimes |\mathbf{k}_2 m_{s_2} m_{t_2}\rangle \otimes ... \otimes |\mathbf{k}_n m_{s_n} m_{t_n}\rangle$$

using Monte-Carlo techniques. Implementation efficient and very transparent.

Drischler, KH, Schwenk, PRL 122, 042501(2019)

Status:

- Implementation of nonlocal NN plus 3N forces up to N3LO complete.
- Implemented MBPT diagrams up to 4th order for NN interactions.
- Generalized to finite T

KH, Krebs, Epelbaum, Golak, Skibinski, PRC 91, 025805 (2015)
Entem et al. PRC 96, 024004 (2017)
Keller et al., arXiv:2011.05855 (2020)

Example: Second order diagram in MBPT

$$E^{(2)}_{\mathrm{NN+3N,eff}} = \frac{1}{4}\left[\prod_{i=1}^{4} \mathrm{Tr}_{\sigma_i} \int \frac{d\mathbf{k}_i}{(2\pi)^3}\right] \left|\langle 12|V^{(2)}_{\mathrm{as}}|34\rangle\right|^2$$
$$\times \frac{n_{\mathbf{k}_1} n_{\mathbf{k}_2}(1-n_{\mathbf{k}_3})(1-n_{\mathbf{k}_4})}{\varepsilon_{\mathbf{k}_1}+\varepsilon_{\mathbf{k}_2}-\varepsilon_{\mathbf{k}_3}-\varepsilon_{\mathbf{k}_4}}(2\pi)^3$$
$$\times \delta(\mathbf{k}_1+\mathbf{k}_2-\mathbf{k}_3-\mathbf{k}_4).$$

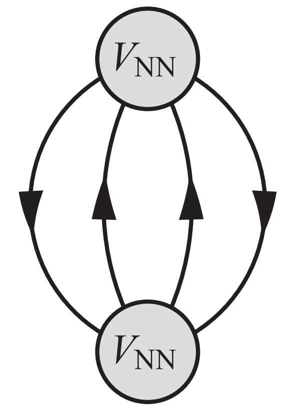

Partial wave representation:

$$\sum_{S,M_S,M_S'} \left|\langle \mathbf{k} S M_S|V^{(2)}_{\mathrm{as}}|\mathbf{k}' S M_S'\rangle\right|^2$$
$$= \sum_L P_L(\cos\theta_{\mathbf{k},\mathbf{k}'}) \sum_{J,l,l',S} \sum_{\widetilde{J},\widetilde{l},\widetilde{l}'} (4\pi)^2 i^{(l-l'+\widetilde{l}-\widetilde{l}')}(-1)^{\widetilde{l}+l'+L}$$
$$\times \mathcal{C}^{L0}_{l0\widetilde{l}'0}\mathcal{C}^{L0}_{l'0\widetilde{l}0}\sqrt{(2l+1)(2l'+1)(2\widetilde{l}+1)(2\widetilde{l}'+1)}$$
$$\times (2J+1)(2\widetilde{J}+1)\begin{Bmatrix} l & S & J \\ \widetilde{J} & L & \widetilde{l}' \end{Bmatrix}\begin{Bmatrix} J & S & l' \\ \widetilde{l} & L & \widetilde{J} \end{Bmatrix}$$
$$\times \langle k|V^{(2)}_{Sl'lJ}|k'\rangle\langle k'|V^{(2)}_{S\widetilde{l}'\widetilde{l}\widetilde{J}}|k\rangle[1-(-1)^{l+S+1}]$$
$$\times [1-(-1)^{\widetilde{l}+S+1}],$$

e.g., KH, Schwenk PRC 82, 014314 (2013)

- hard to automatize and generalize to higher order diagrams
- prone to mistakes

Single-particle vector representation:

$$\frac{E^{(2)}_{\mathrm{NN}}}{V} = +\frac{1}{4}\sum_{\substack{ij\\ab}} \frac{\langle ij|\mathscr{A}_{12}V_{\mathrm{NN}}|ab\rangle\,\langle ab|\mathscr{A}_{12}V_{\mathrm{NN}}|ij\rangle}{D_{ijab}}$$

- each diagram just a few lines of code
- straightforward to automatize code generation
- adaptive evaluation of integrals using Monte-Carlo techniques
- allows inclusion of 3N contributions without normal ordering

High-order calculations of nuclear matter

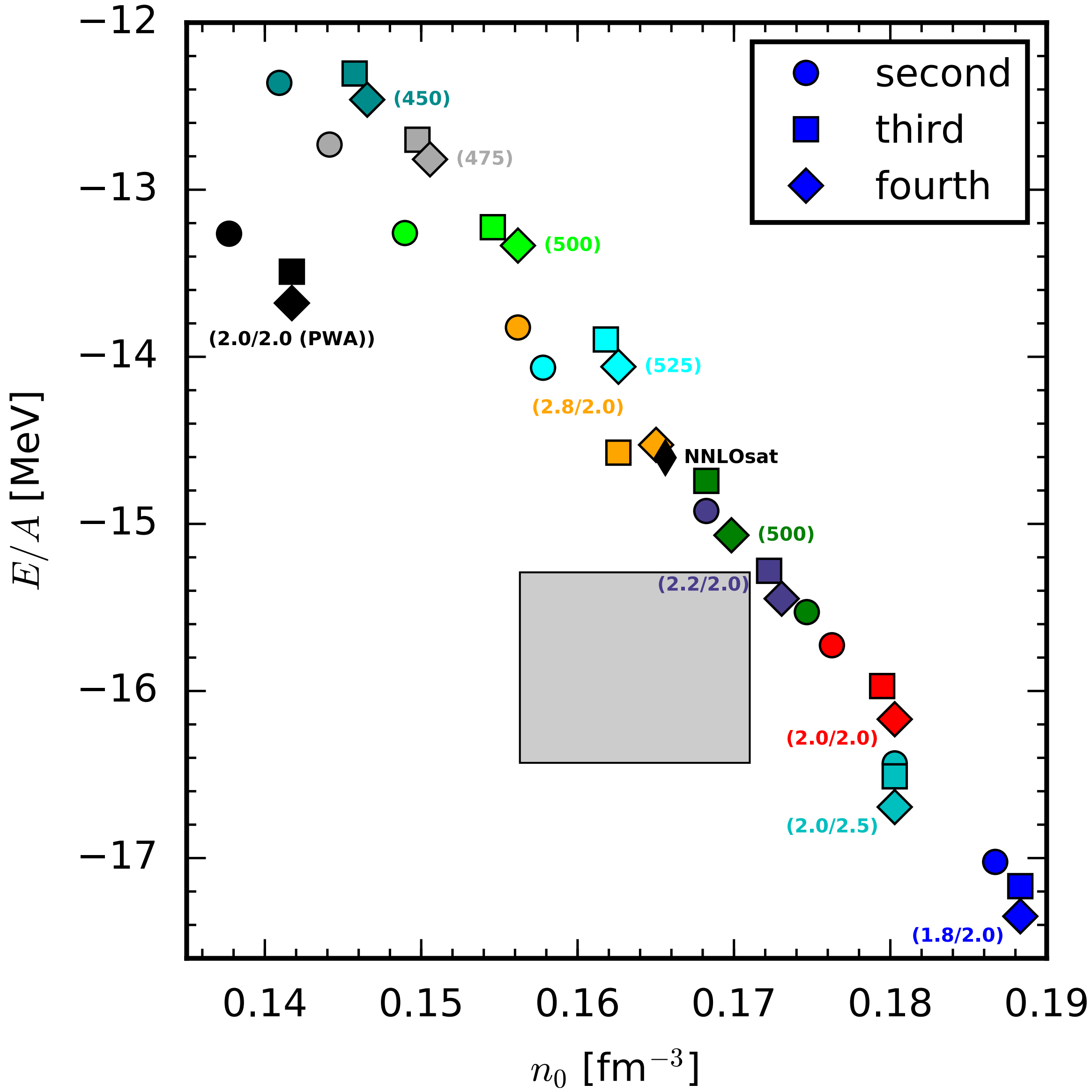

Drischler et al.,
PRL 122, 042501(2019)

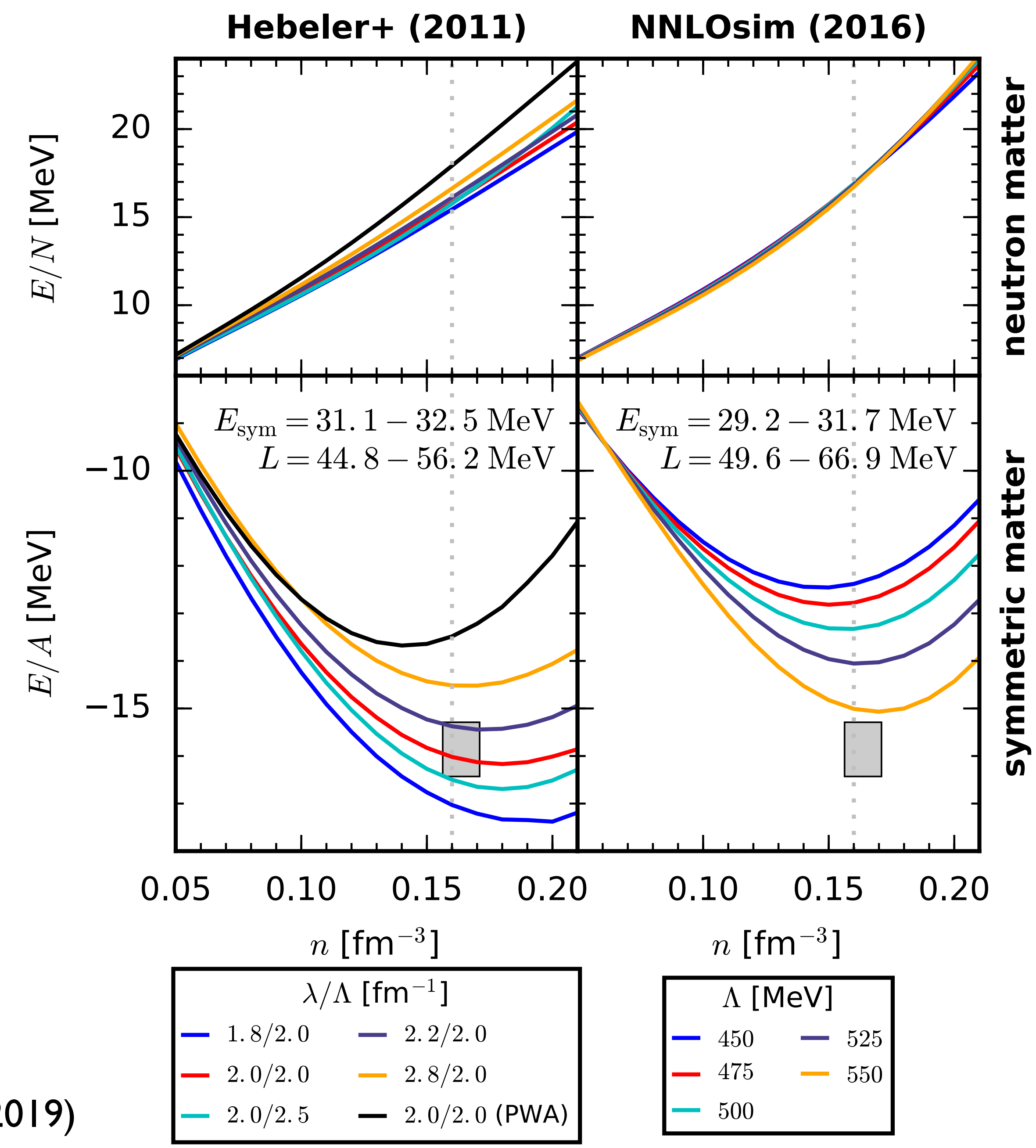

- state-of-the-art NN plus 3N interactions exhibit a systematic trend for saturation point (similar to Coester line)
- first incorporation of saturation properties in fits of 3N interactions

Uncertainty estimates from EFT truncation

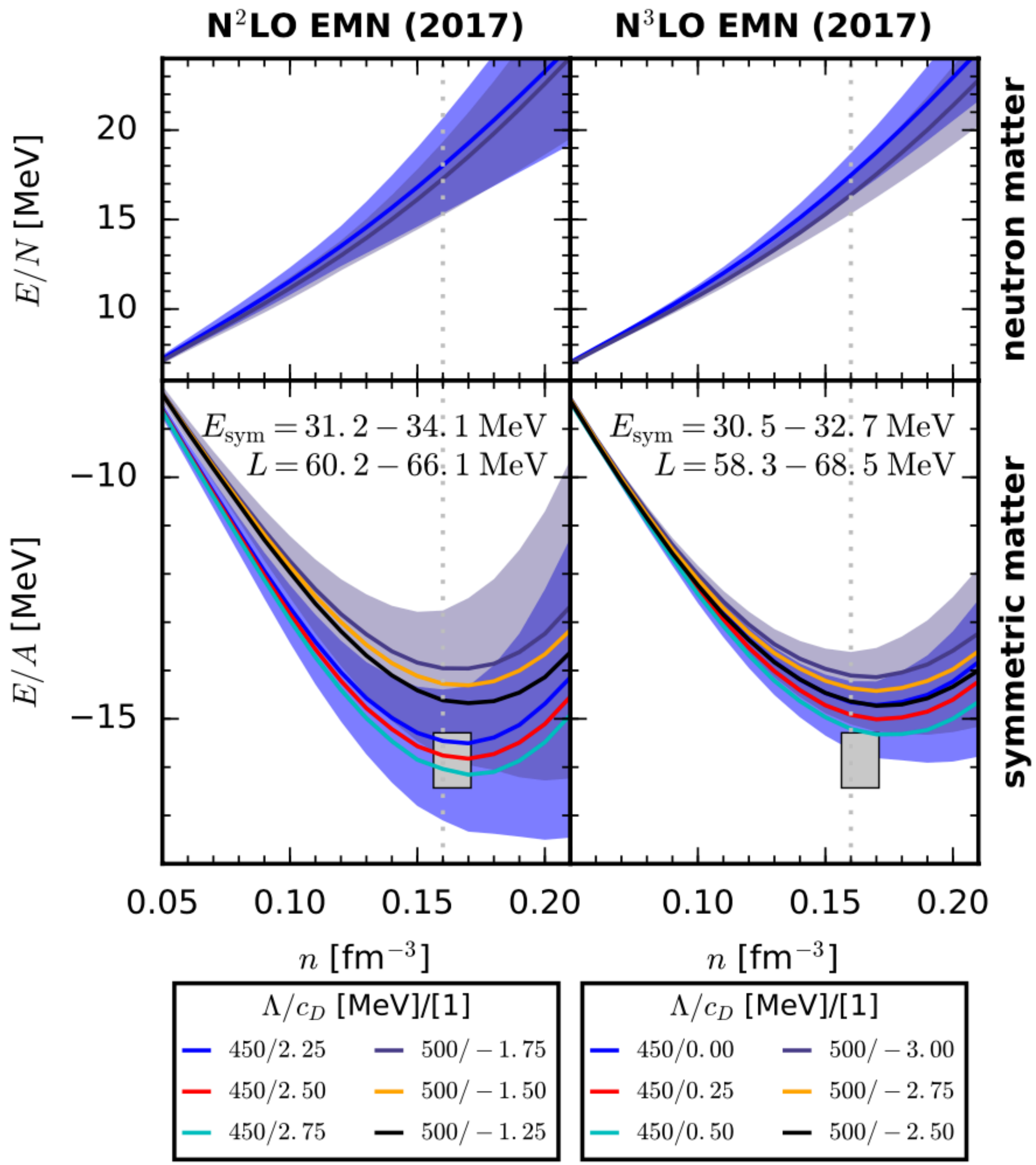

- uncertainty bands determined from chiral EFT order-by-order calculations

Epelbaum et al., EPJA 51, 53 (2015)

- uncertainty estimates validated by a Bayesian analysis

Drischler et al., PRL 125, 20 (2020)
Drischler et al., PRC 102, 054315 (2020)

Asymmetric nuclear matter EOS

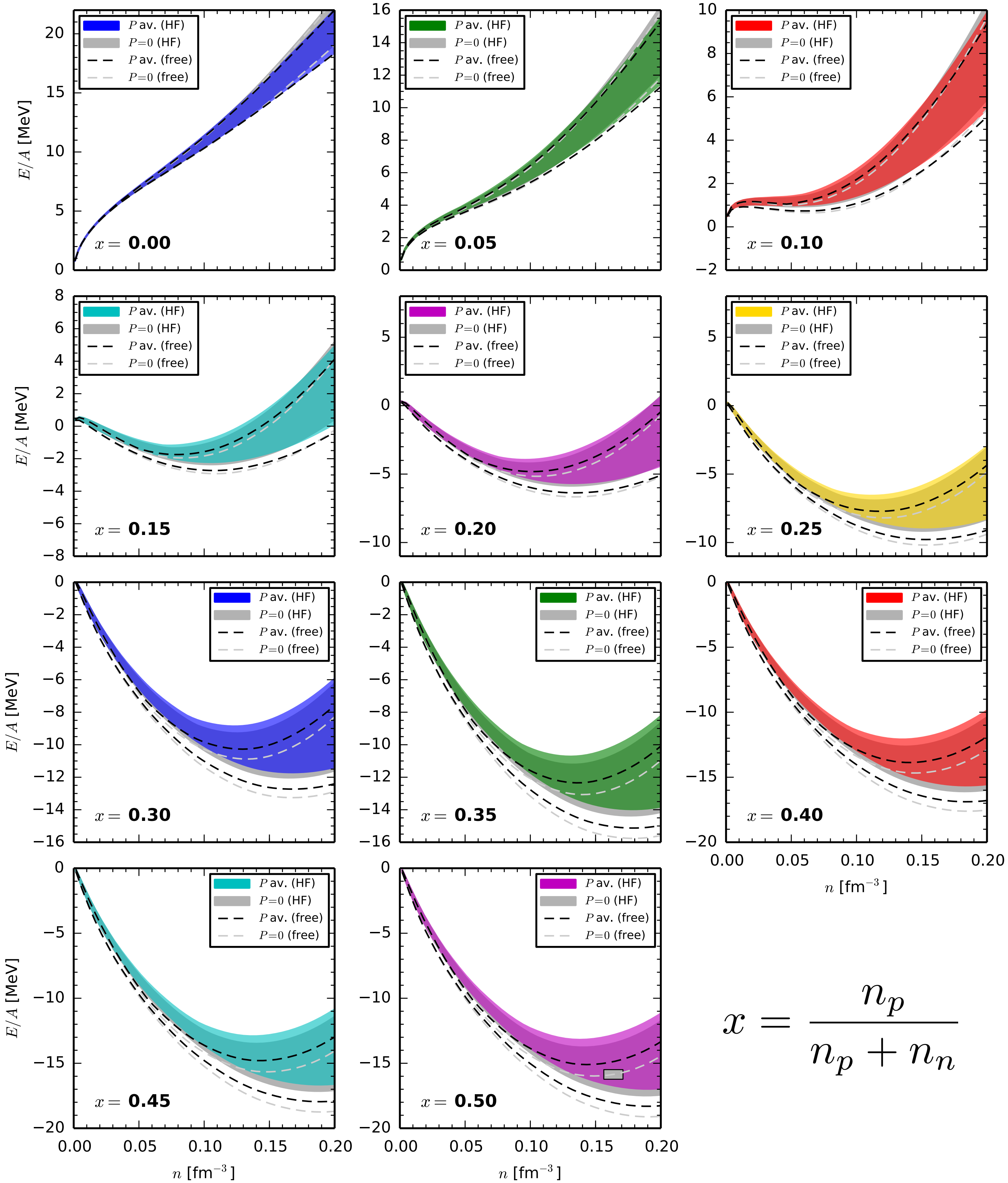

$$x = \frac{n_p}{n_p + n_n}$$

- microscopic framework to calculate equation of state for general proton fractions
- uncertainty bands determined by set of 7 Hamiltonians

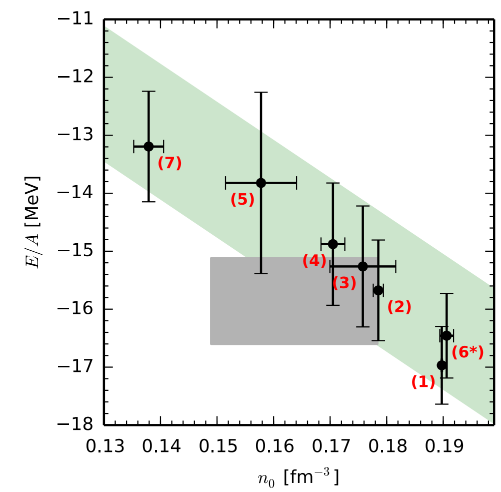

- many-body framework allows treatment of general 3N interaction

Drischler, KH, Schwenk, PRC 054314 (2016)

High-density constraints for the EOS

constraining EOS at high densities by calculations or astrophysical observations

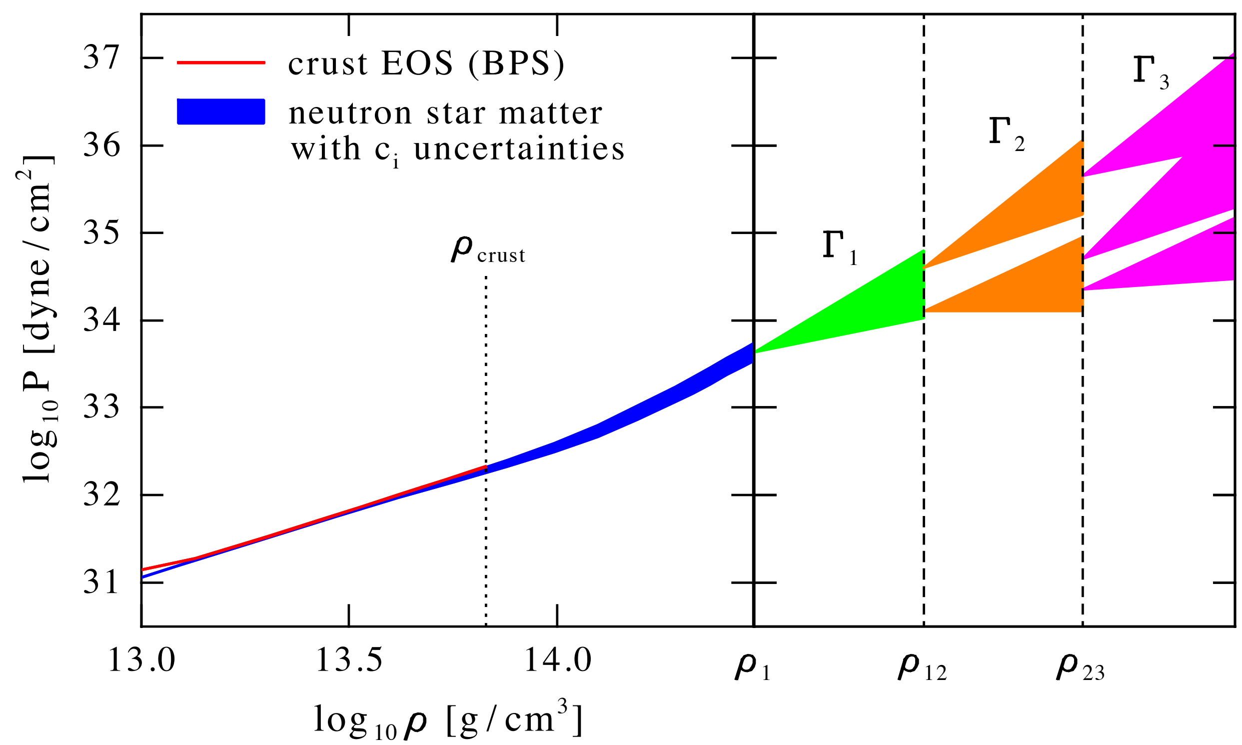

KH, Lattimer, Pethick, Schwenk, ApJ 773, 11 (2013)

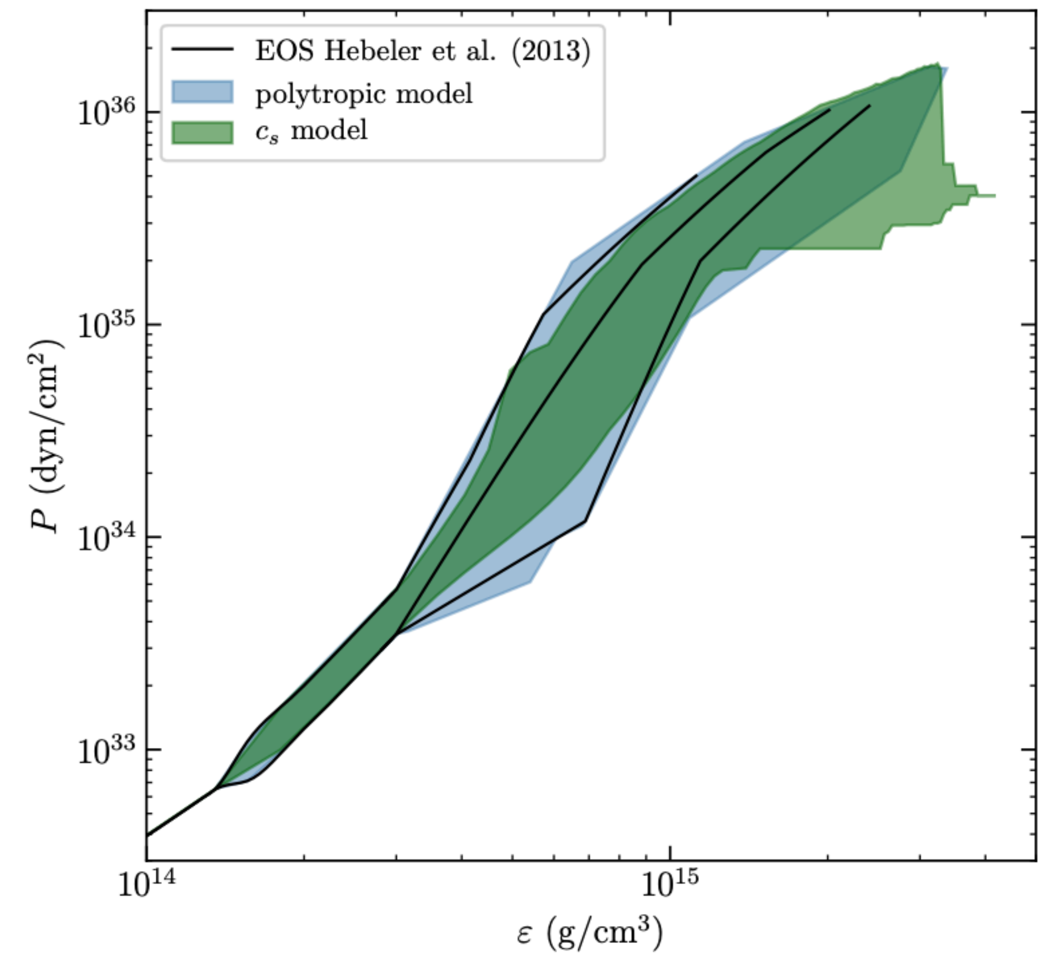

Greif et al., MNRAS 485, 5363 (2019)

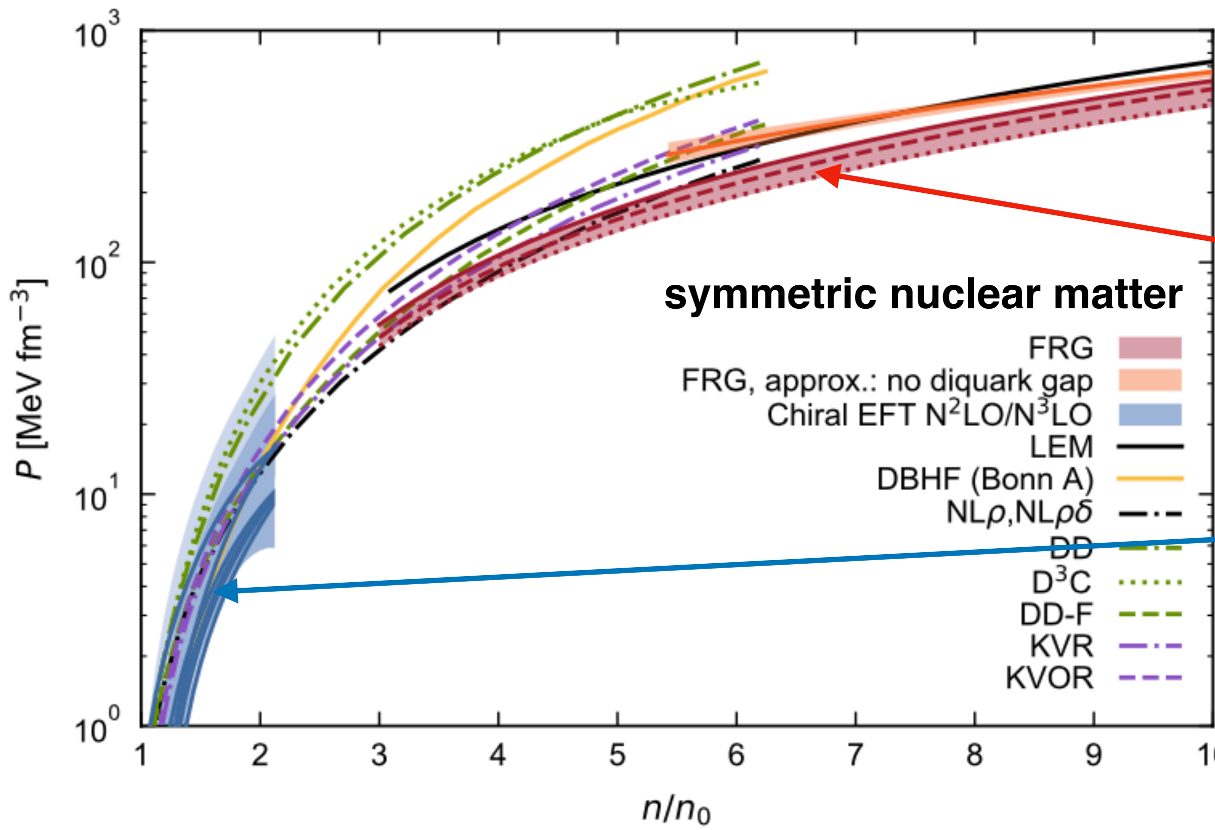

- QCD-functional renormalization group equation calculations
- encouraging consistency with chiral EFT results at low densities

Leonhardt et al., PRL 125,142502 (2020)

The equation of state of high-density matter: constraints from neutron star observations

- observation of heavy neutron stars

  Demorest et al., Nature 467, 1081 (2010)
  Antoniadis et al., Science 340, 448 (2013)
  Cromartie et al., Nature Astron. 4, 72 (2020)

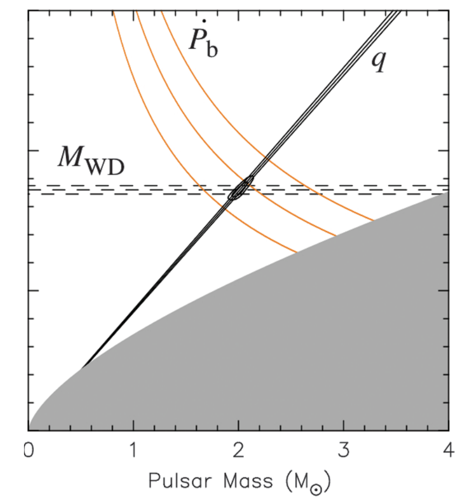

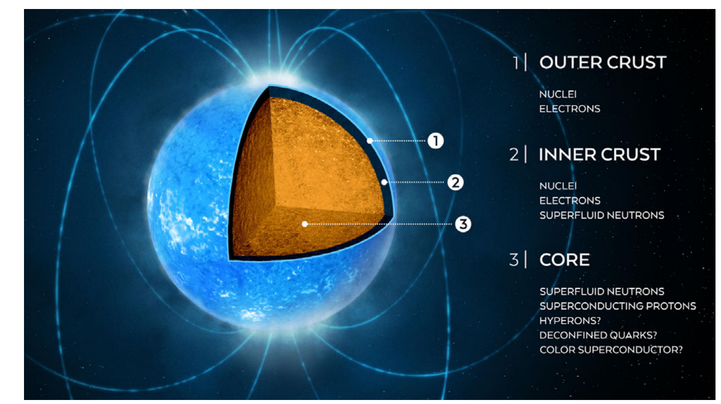

- detection of gravitational waves from neutron star merger event

  Abbott et al., PRL 119, 161101 (2017)

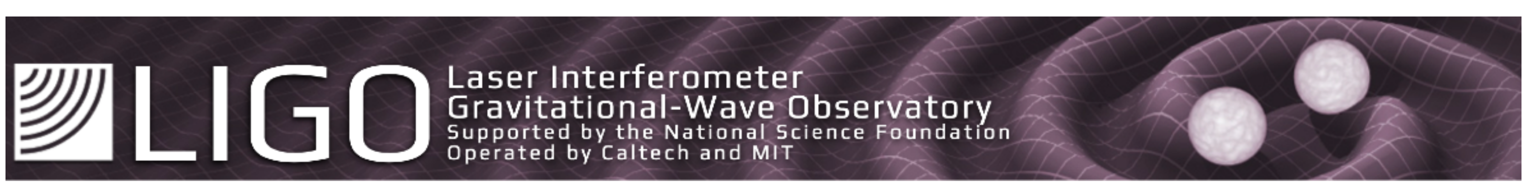

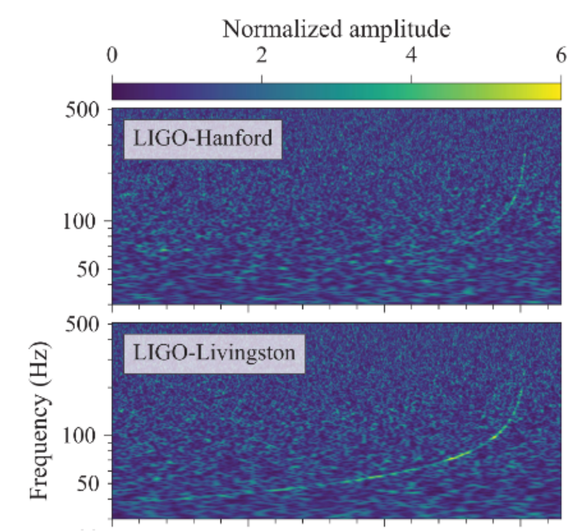

- radius measurements from pulsar x-ray timing

  Watts et al., RMP 88, 021001 (2016)
  Riley at al., APJL 887, 21 (2019)
  Raaijmakers et al., APJL 887, 22 (2019)

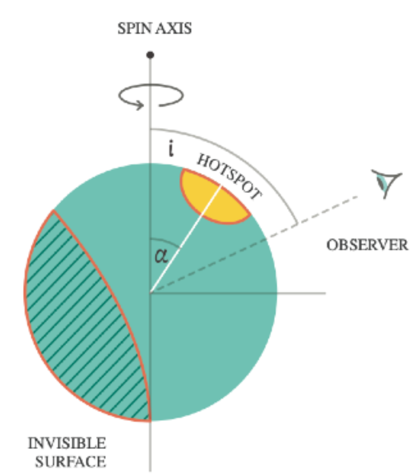

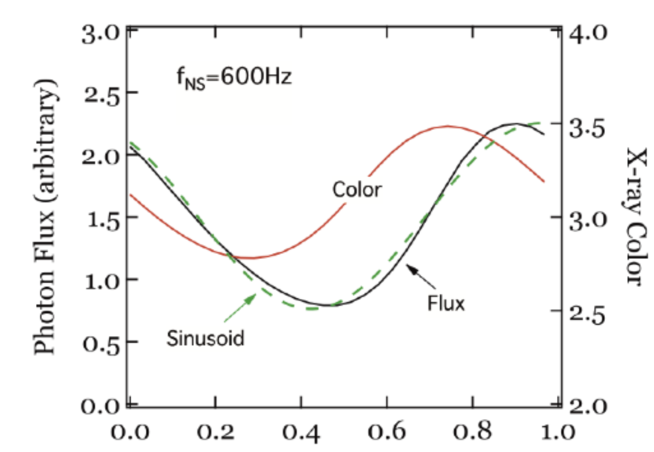

Constraints on neutron star radii

constraints on EOS and NS radii from first NICER observations:

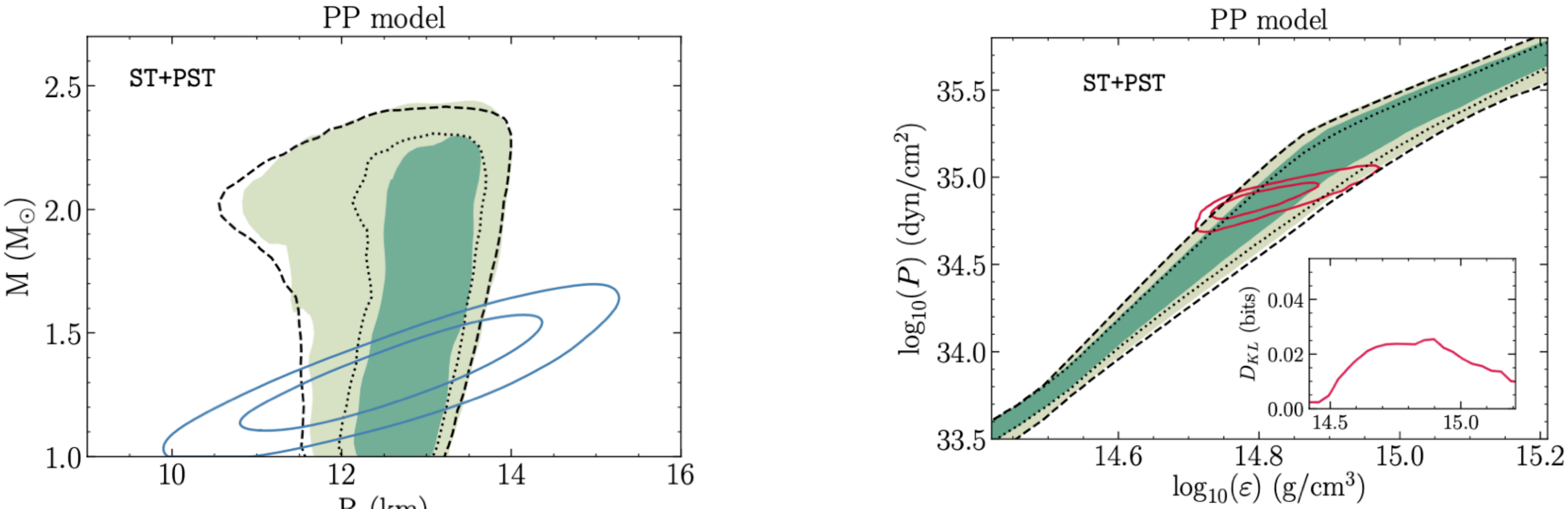

Raaijmakers et al., APJL 887, 22 (2019)

additionally incorporating constraints from LIGO and mass measurements:

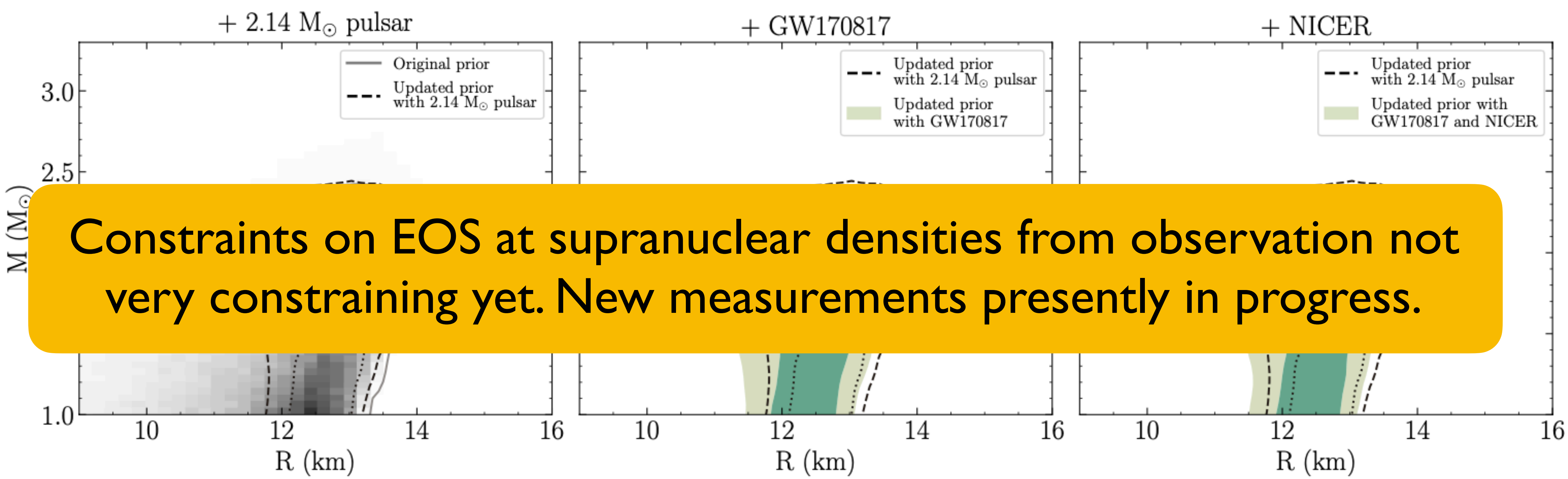

Constraints on EOS at supranuclear densities from observation not very constraining yet. New measurements presently in progress.

Neutron matter at finite temperature

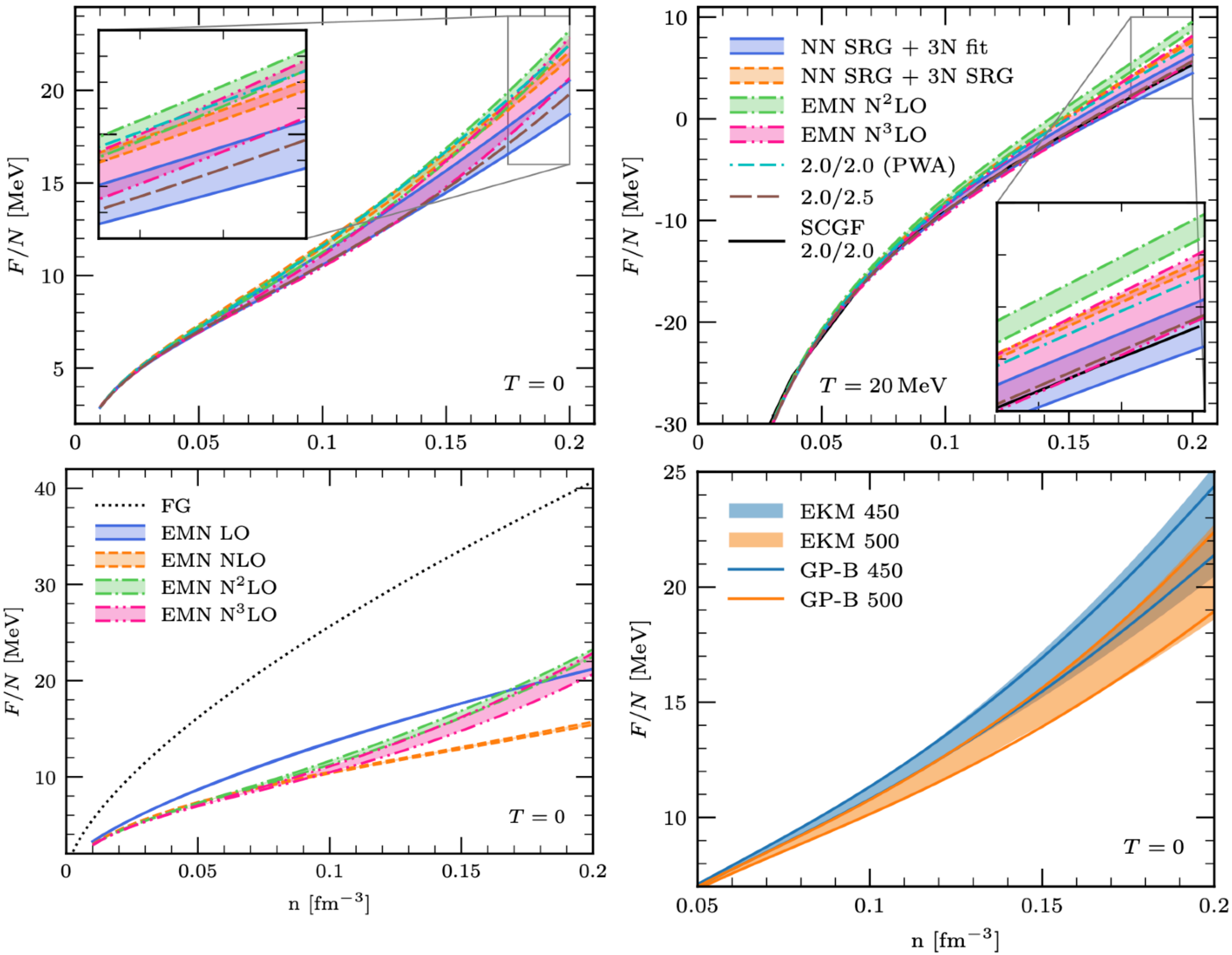

Jonas Keller

Keller et al., arXiv:2011.05855 (2020)

- calculations based on a set of state-of-the-art NN plus 3N interactions
- order-by-order results in chiral expansion and resulting uncertainty estimates

Neutron matter at finite temperature

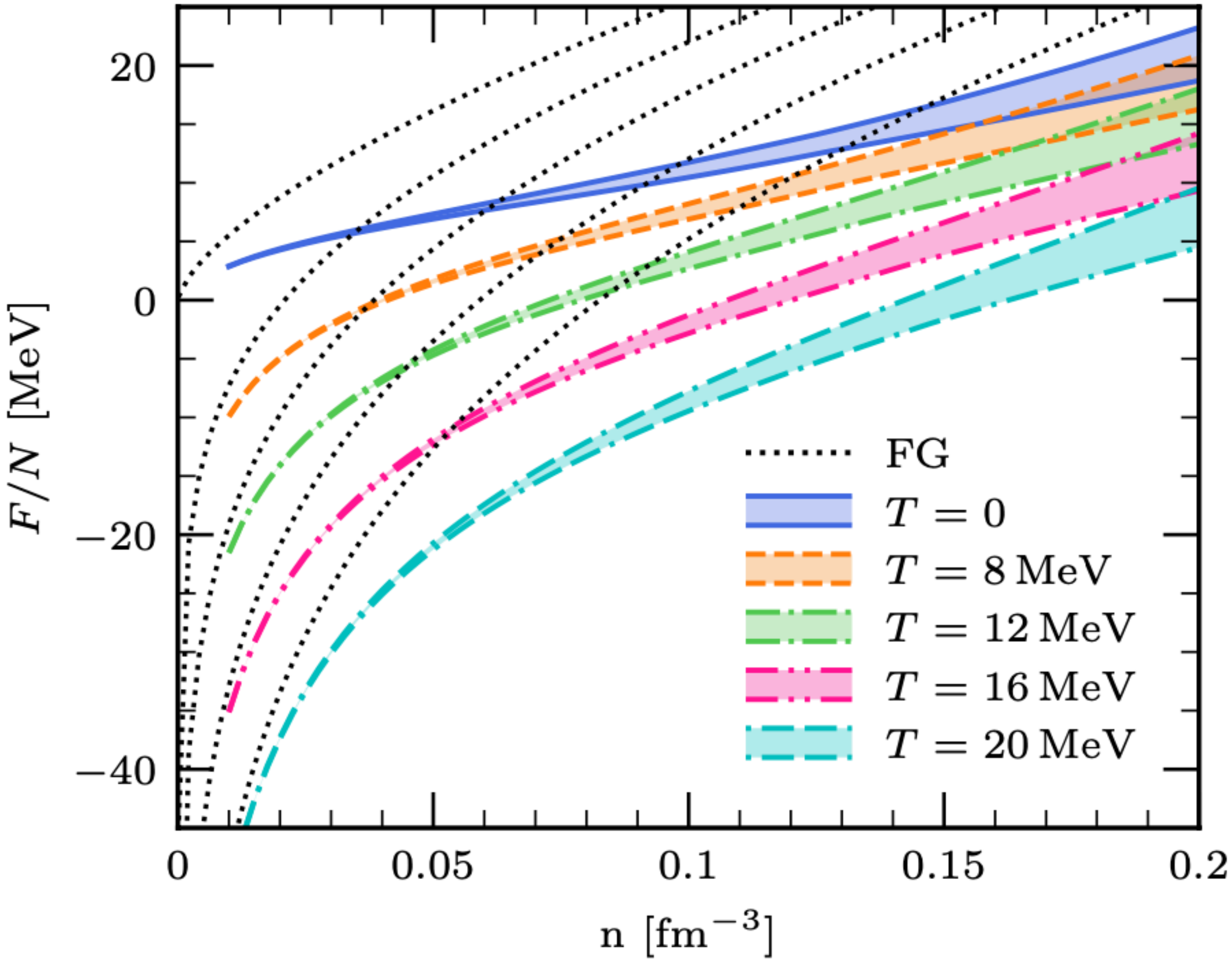

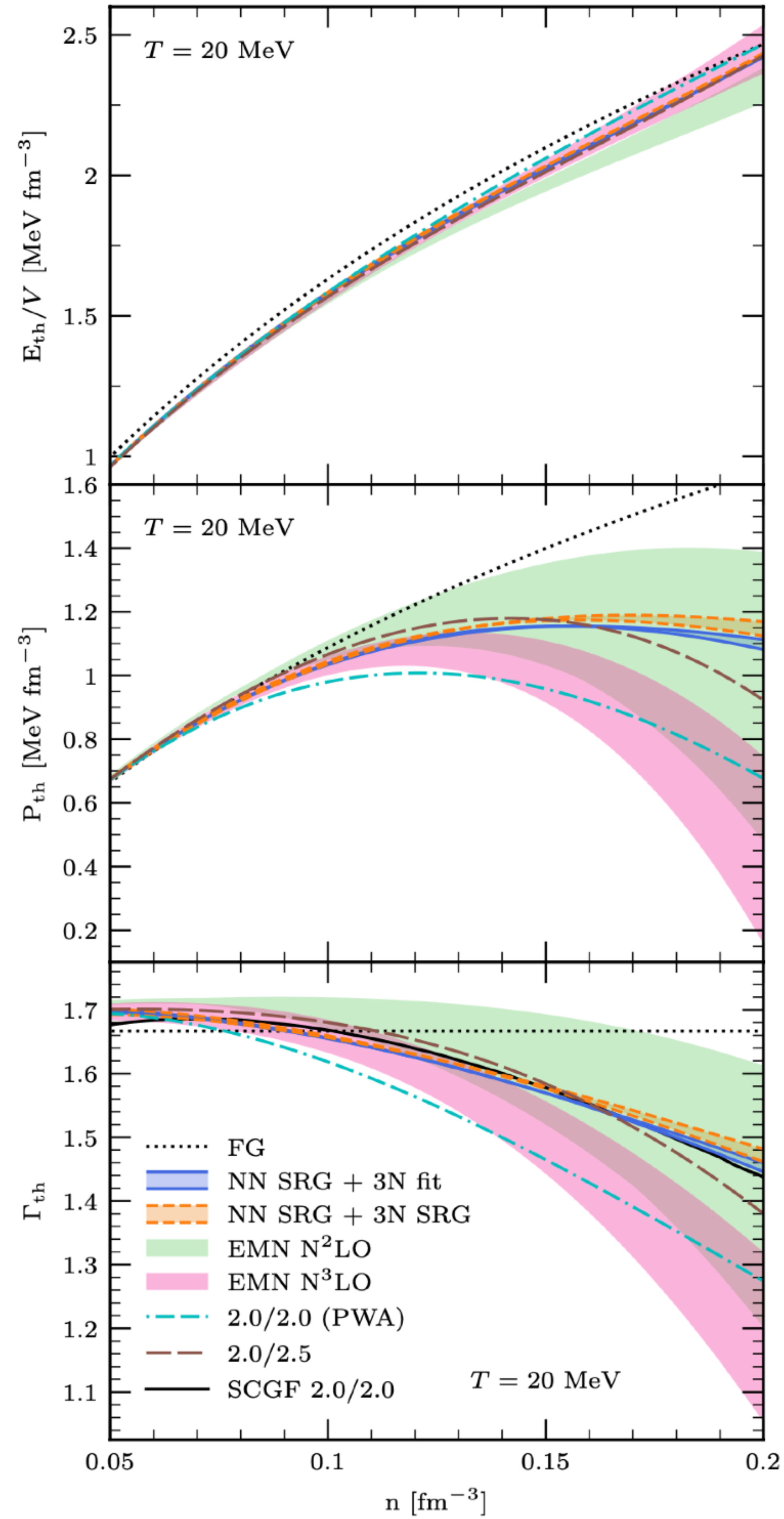

Thermal contributions and thermal index

$$X_{\text{th}}(T,n) = X(T,n) - X(T=0,n)$$

$$\Gamma_{\text{th}}(T,n) = 1 + P_{\text{th}}(T,n)/\mathcal{E}_{\text{th}}(T,n)$$

Further steps

- generalisation of framework to general isospin-asymmetric matter
- optimisation of 3N handling for increased accuracy of calculations
- high-density QCD calculations for neutron-rich matter (J. Braun's group, TU Darmstadt) ⟶ combination with chiral EFT results

Discussion points

- How to include uncertainty bands in COMPOSE files?
- Additional observables of interest for astrophysical applications?